Oil Shale, 2013, Vol. 30, No. 3, pp. 377–401
doi: 10.3176/oil.2013.3.02
ISSN 0208-189X

GEOCHEMICAL HETEROGENEITY OF ESTONIAN GRAPTOLITE ARGILLITE

MARGUS VOOLMA*, ALVAR SOESOO, SIGRID HADE, RUTT HINTS, TOIVO KALLASTE

Institute of Geology, Tallinn University of Technology, Ehitajate tee 5, 19086 Tallinn, Estonia

Abstract. *This paper describes vertical fine-scale geochemical heterogeneity of Estonian graptolite argillite (GA). GA samples from Pakri and Saka outcrop sections were collected at 20 cm intervals for chemical analysis of major and trace elements, including rare earth elements. The study indicates GA enrichment in U, V, Mo and Pb with respect to the average black shales and thus confirms the formerly reported data on GA geochemistry in general. However, the content of enriched elements and other trace metals was recorded to vary greatly across the sequences suggesting that trace metal distribution in GA is notably more heterogeneous than previously assumed. The origin of the observed complex distribution of trace elements was likely controlled by the interplay of different primary metal supply-sequestration factors/processes, such as synsedimentary redox-driven sequestration of redox sensitive elements, the provenance of clastic input, the post-sedimentary redistribution, etc.*

Keywords: *graptolite argillite, black shale, geochemistry, trace metals, REE, Estonia.*

1. Introduction

The Estonian graptolite argillite (GA), Tremadoc in age, is distributed in northern Estonia and on Vormsi and Hiiumaa islands. It belongs to the Türisalu Formation and is overlain by glauconitic sandstones and clays of the Varangu Stage and underlain by the phosphatic quartzose sandstone of the Kallavere Formation [1]. The GA is an argillaceous rock enriched with organic matter [2] and is characterized by high concentrations of a number of trace elements, including U, V and Mo. The thickness of GA reaches 7.4 m in NW Estonia and decreases towards the east and south. On a regional scale, GA belongs to the wide but patchy belt of Middle Cambrian

* Corresponding author: e-mail *voolma@gi.ee*

to Lower Ordovician black shales extending from Lake Onega district in the east to the Caledonian front, Oslo region and Jutland Peninsula in the west [3–6].

There are numerous studies conducted on various metalliferous black shale/oil shale deposits worldwide – black shale deposits in North America [7–12], China [13, 14], central Europe [15], and alum shale in Scandinavia [3, 16–20] – focusing on the general characteristics and different aspects of metallogenesis in those assemblages. Also, a series of investigations have been targeted on the general geochemistry and trace element distribution of Estonian GA [21–30].

The metalliferous nature of GA was well known already in the first half of the last century. A more systematic picture of GA outside its outcrop area near the Baltic Klint, however, was gathered thanks to the extensive geological mapping of basement, drilling and geochemical investigations, which started in the 1950s and were conducted by the Geological Survey of Estonia. The vast amount of detailed information on the GA lithology and geochemistry was collected during the prospecting of Estonian phosphorite resources, e.g. [23, 31, 32]. The previous investigations have allowed depicting general trends of trace element enrichment and lateral distributions within GA, demonstrating at the same time high trace metal heterogeneity of those deposits [26, 28, 29]. Still, relatively little is known about the source of metals and the mechanism that caused metal enrichment in many black shale deposits worldwide, including GA. Although several investigations have been conducted during the past decades [25–30], the origin of metals is still unclear, as why their content is so heterogeneous laterally and also vertically through the GA complex.

Based on previous geochemical investigations [26] three geochemical zones have been distinguished in Estonian GA: Western, Central and Eastern zones (Fig. 1). The zones differ mainly in concentration of metals which are characteristic of GA – Mo, V, U. However, based on the present study it will be shown that the distribution of metals in GA has a more complex pattern. This paper describes the vertical bed-to-bed variation of metals, with emphasis on two vertical cross-sections, and discusses some possible critical factors that may stand behind the trace metal enrichment and heterogeneity in those complexes. Samples for the study were collected from Pakerort cliff on Pakri Peninsula, NW Estonia and Saka cliff, NE Estonia (Fig. 1), selected to represent GA complex in different geochemical zones. According to biostratigraphic studies GA in those localities does not represent strictly coeval sedimentation: GA from Western Estonia is assigned to the Pakerort Stage, whereas GA within the Eastern Zone belongs to the younger Varangu Stage [33, 34].

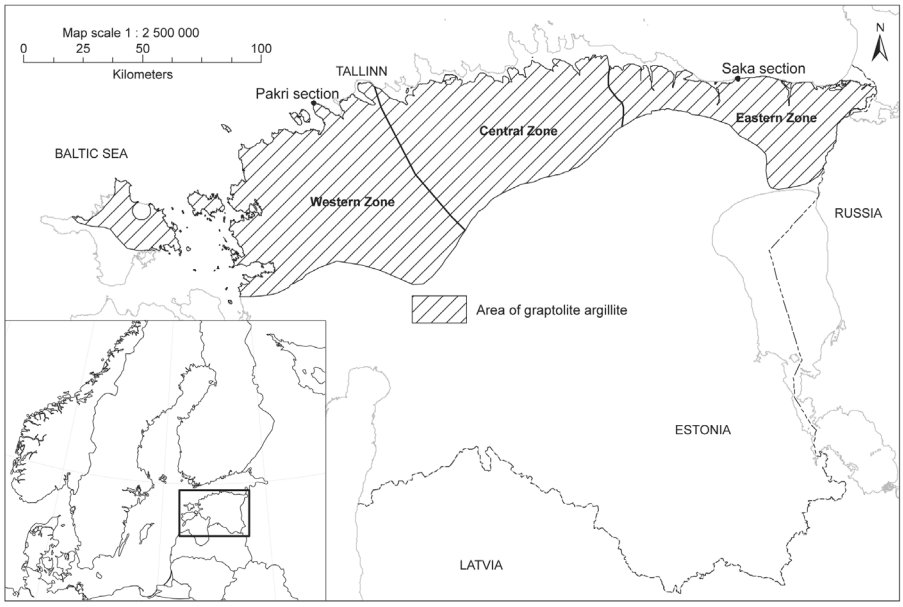

Fig. 1. Map of the location of GA and sampled outcrop sections.

2. Material and methods

Two outcrops, Pakri and Saka, were sampled at 20 cm intervals for geochemical analysis. Twenty-one fresh GA samples from Pakri and nine samples from Saka were collected from the outcrop sections of 4.2 m and 1.8 m, respectively. The weight of samples was approximately 2 kg. The samples were cleaned, dried, crushed and homogenized for chemical analysis. The sample powders were analyzed for major and trace element composition, including rare earth elements, in order to determine the geochemical changes across the section and general rock composition. Geochemical analysis was performed using X-ray fluorescence (XRF) and ICP-MS analysis.

XRF analysis was conducted at the Institute of Geology, Tallinn University of Technology (TUT), with an S4 Pioneer Spectrometer (Bruker AXS GmbH, Germany), using an X-ray tube with a rhodium anode, which operated with a power of 3 kW. The samples were measured with a manufacturer's standard as MultiRes modification (pre-calibrated standardless method). The in-house standard ES-2 ("Dictyonema Shale") was used as reference material [34]. Loss on ignition (LOI) was determined from 1 g of sample material at 500 °C and 920 °C. ICP-MS analysis was conducted at the Institute of Geology, TUT. Rare earth elements of Pakri samples were determined from solutions which were prepared following the nitric, hydrofluoric, hydrochloric and boric acids digestion of a 0.250 g pulverized sample in an Anton Paar MW3000 microwave oven. A set of samples from

Pakri and Saka were additionally re-analyzed for trace elements, including rare earths, at ACMELABS in Canada.

Mineralogical analysis of selected whole rock powdered samples was conducted using an X-ray diffractometry apparatus (HZG4 diffractometer) at the Institute of Geology, TUT. XRD analysis was performed using a Fe-filtered Co radiation (35 kV and 25 mA) and scintillation detector. The range from 5–45°2Θ was scanned with a step of 0.04°2Θ. For selected samples complementary scanning electron microscope (SEM) analysis was used. SEM examination of uncoated rough and flat unpolished GA samples was carried out at the Institute of Geology, TUT, with a Zeiss EVO MA15 scanning electron microscope.

3. Mineralogy of graptolite argillite

GA is a fine-grained kerogen-rich siliceous deposit characterized by high content of organic matter (15–20%) and pyrite (2.4–6.0%) [2], and very low thermal maturity. The mineral assemblage of GA is according to previous studies dominated by K-feldspars, quartz and clay minerals [35, 36]. In the lateral as well as vertical dimension the contents of major rock-forming minerals show slight but pronounced variation patterns [35, 37, 36]. The average content of quartz in GA gradually rises eastward with the corresponding clay mineral decrease. In NE Estonia, the argillite complex is intercalated with numerous quartzose silt beds [30]. From authigenic sulfides, the occurrence of pyrite, marcasite, sphalerite and galena has been documented. In outcrops and drill cores secondary gypsum and jarosite commonly appear. In general, a higher degree of sulfide mineralization within GA is associated with the occurrence of silt interbeds. Those interbeds might also host a higher amount of other minor authigenic compounds typical for GA – phosphates (mainly apatite as biogenic detritus and nodules), carbonates (calcite and dolomite as cement and concretions), barite and glauconite. Besides the highly resistant terrigenic accessory phases, considerable abundance of micas in GA beds has been documented [35, 37].

Detailed mineralogical study is beyond the scope of the present paper. However, in order to record general mineralogical outline, XRD analysis of selected GA samples from the Pakri outcrop was performed. The study confirmed the presence of K-feldspar (sanidine), illite (illite-smectite, micas), quartz, pyrite, marcasite, apatite, calcite, dolomite, galena and chlorite. The analysis with SEM revealed high micrometer-scale morphological heterogeneity in the examined samples. The dominance of finely disseminated microcrystalline euhedral K-feldspar and quartz in argillite suggests that these minerals in GA are commonly authigenic in origin. The multistage development of syngenetic-diagenetic mineral assemblages and importance of redistribution processes in GA are suggested by the

occurrence of a high variety of pyrite crystal forms within the argillite matrix as well as in sulfide enriched interbeds.

4. Results and discussion on the geochemistry of the Estonian graptolite argillite

Detailed vertical geochemical heterogeneity in the GA has not been studied previously. There is little understanding of the scale of heterogeneity and distribution pattern of elements. Moreover, detailed lateral geochemical changes across the GA unit are unknown. As an example of elemental distribution, V, Mo and Pb within the Estonian GA unit are displayed in Figure 2. The initial data were selected from the database of the Geological

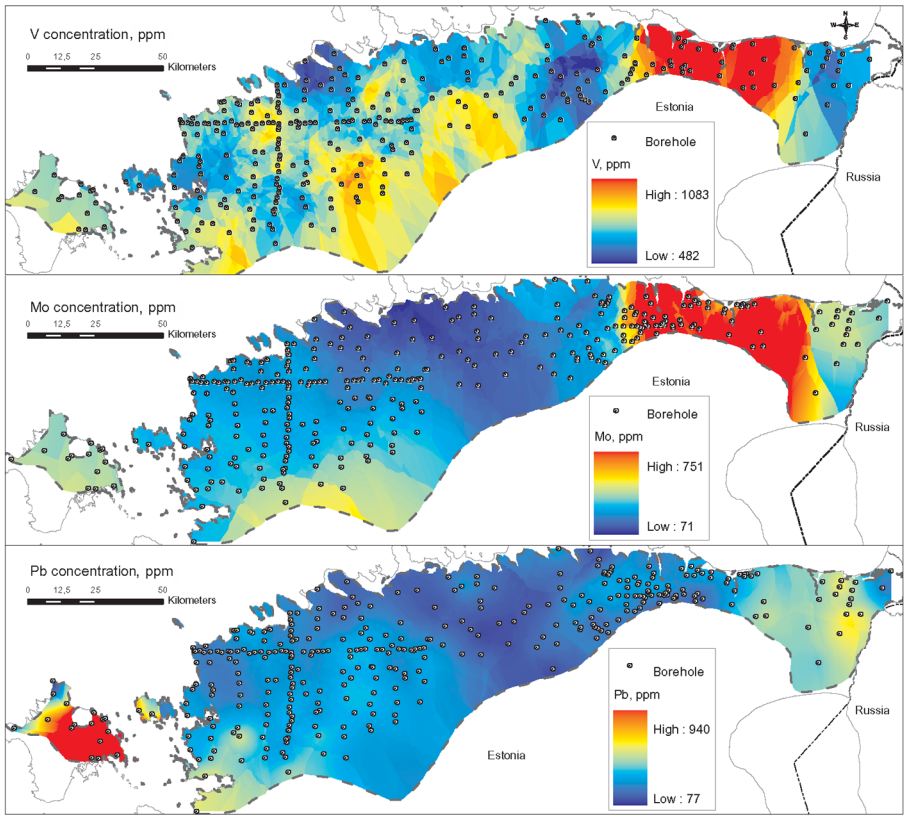

Fig. 2. V, Mo and Pb concentrations in Estonian GA as modeled using calculated average drill core analyses (data: Geological Survey of Estonia, 2008). Element concentration surfaces were modeled by the kriging method using spherical distances (ESRI ArcGIS). For distribution model of V data from 297 drill cores were selected, for Mo 325 and for Pb 345 drill cores were used.

Survey of Estonia. These elemental concentration data represent the calculated average concentration in the GA in the drill core. The central and western parts of the Eastern Zone show the highest concentrations for V and Mo (Figs. 2, 1). Generally, it can be concluded that the concentration of most of the metals is relatively low in the Central Zone (Figs. 2, 1). Pb shows the highest concentrations on Hiiumaa Island. It must be emphasized that the available data is relatively unevenly distributed, especially the southern margin of the GA bed. Therefore, geochemical generalizations of this kind are informative but must be taken with precaution. More drilling material and studies of the vertical geochemical change of elements in GA are needed to define spatial geochemical patterns.

4.1. Major elements

The bed-to-bed study performed on geochemical variation from Saka and Pakri sections show that major elements vary relatively little across the examined GA sequences (Table 1). Analyses indicate that the GA assemblage is siliceous, high-K, Mn-poor and with variable Fe and S contents.

The SiO_2 abundance in examined GA sections varies from 45.74 to 55.11 wt% and shows a general increase towards the upper part of the GA complex. The observed distribution pattern agrees with previously described lithological changes – general increase of the silt/clay ratio from bottom to top of the beds in Estonian GA sequences [37, 36]. Besides, there is an inverse correlation between LOI 500 °C (reflecting organic matter content in GA) and SiO_2. The Al_2O_3 content varies between 10.9 and 14.49 wt% and its average concentration is somewhat higher in GA from the Pakri locality. Titanium behavior shows a strong correlation with aluminum suggesting a possible detrital origin. The distinct feature of the Estonian GA is its elevated potassium content, in Pakri and Saka GA sequences K_2O ranges from 6.59 to 8.44 wt%. The high potassium content is likely connected with the abundance of authigenic K-feldspar in those beds, thus differentiating Estonian GAs from the Scandinavian alum shale, where clay minerals occur as the dominant K-rich phases [38]. Pronounced potassium enrichment is also evident when the detected chemical composition of GA is compared with the compositions of widely used standard shale compilations such as PAAS (Post Archaean Australian Shale) [39], and NASC (North American Shale Composite) [40] (Fig. 3). On the other hand, a number of major element compounds, such as MnO, Na_2O, CaO, MgO, appear to be considerably depleted with respect to the "standard shale" composition. The content of all those elements in the studied GA sequences is consistently well below 1.5 wt%.

The invariably low manganese content of Cambrian-Tremadoc black shales of the Baltoscandian region was interpreted by Wilde et al. [10] as an indicator of persistently euxinic environment during accumulation of the

Table 1. Major elements in GA samples from Pakri and Saka sections

Interval, cm			GI XRF %												%	GI %	
From	To	Sample	SiO_2	TiO_2	Al_2O_3	Fe_2O_3	MnO	MgO	CaO	Na_2O	K_2O	P_2O_5	Cl	S	SUM	LOI500°C	LOI920°C
0	20	Pakri1	46.10	0.72	13.91	4.89	0.020	1.31	0.25	0.07	8.00	0.15	0.019	2.23	99.48	22.10	24.05
20	40	Pakri2	45.74	0.71	13.60	4.01	0.020	1.33	0.22	0.07	7.77	0.11	0.020	1.96	99.69	24.46	26.09
40	60	Pakri3	46.83	0.70	13.55	4.29	0.019	1.30	0.20	0.07	7.73	0.12	0.026	2.11	99.69	23.27	24.86
60	80	Pakri4	48.77	0.72	13.66	4.33	0.020	1.27	0.23	0.06	7.95	0.14	0.022	2.16	99.16	20.46	21.99
80	100	Pakri5	48.01	0.72	13.60	4.44	0.020	1.26	0.13	0.06	7.82	0.12	0.025	2.11	99.54	21.77	23.33
100	120	Pakri6	47.57	0.72	13.38	4.07	0.019	1.22	0.12	0.06	7.85	0.10	0.023	2.02	98.87	22.21	23.73
120	140	Pakri7	48.37	0.73	13.65	4.13	0.018	1.22	0.11	0.07	7.92	0.12	0.029	2.03	99.59	21.69	23.22
140	160	Pakri8	49.91	0.75	13.85	4.36	0.019	1.23	0.10	0.07	8.02	0.12	0.023	2.12	99.87	19.79	21.42
160	180	Pakri9	48.25	0.73	13.85	4.28	0.018	1.23	0.12	0.06	8.12	0.09	0.024	2.16	99.99	21.59	23.22
180	200	Pakri10	49.63	0.70	13.45	4.95	0.017	1.17	0.16	0.06	7.88	0.14	0.018	2.56	99.54	19.73	21.36
200	220	Pakri11	51.35	0.75	13.94	4.97	0.017	1.18	0.15	0.07	8.25	0.18	0.020	2.39	99.70	16.96	18.83
220	240	Pakri12	49.71	0.75	13.65	4.25	0.018	1.19	0.13	0.07	8.12	0.14	0.023	2.08	99.03	19.30	20.99
240	260	Pakri13	49.09	0.74	13.67	5.22	0.019	1.25	0.14	0.07	7.77	0.13	0.017	2.64	100.03	19.95	21.92
260	280	Pakri14	49.41	0.74	13.88	6.08	0.018	1.25	0.21	0.07	7.72	0.19	0.017	2.98	99.98	18.45	20.40
280	300	Pakri15	49.61	0.76	14.06	4.38	0.019	1.30	0.18	0.07	8.20	0.13	0.018	2.06	99.02	18.60	20.29
300	320	Pakri16	48.97	0.75	14.00	4.44	0.018	1.24	0.10	0.07	8.15	0.13	0.019	2.18	99.15	19.50	21.27
320	340	Pakri17	52.43	0.68	13.21	4.25	0.019	1.16	0.60	0.07	7.91	0.48	0.015	2.14	98.18	15.40	17.35
340	360	Pakri18	50.03	0.79	14.49	4.21	0.021	1.33	0.18	0.07	8.44	0.14	0.017	1.95	100.12	18.58	20.40
360	380	Pakri19	51.69	0.80	14.41	4.42	0.021	1.33	0.23	0.07	8.42	0.17	0.013	1.95	99.20	15.83	17.62
380	400	Pakri20	51.87	0.78	14.12	4.72	0.020	1.23	0.18	0.07	8.32	0.11	0.014	2.23	99.33	16.10	17.89
400	420	Pakri21	51.59	0.79	14.09	5.02	0.022	1.27	0.43	0.08	8.16	0.27	0.015	2.41	99.49	15.30	17.76
0	20	Saka1	49.73	0.73	11.94	4.21	0.009	0.72	0.25	0.06	7.23	0.37	0.020	2.68	99.99	21.28	24.73
20	40	Saka2	51.75	0.64	11.00	6.00	0.008	0.64	1.08	0.06	6.59	1.08	0.019	4.00	99.29	16.03	20.43
40	60	Saka3	48.28	0.64	11.27	4.20	0.009	0.67	0.18	0.05	6.90	0.54	0.028	2.57	99.05	23.70	26.29

Table 1 (continuation)

Interval, cm			GI XRF %												%	GI %	
From	To	Sample	SiO_2	TiO_2	Al_2O_3	Fe_2O_3	MnO	MgO	CaO	Na_2O	K_2O	P_2O_5	Cl	S	SUM	LOI500°C	LOI920°C
60	80	Saka4	46.54	0.68	11.84	3.93	0.012	0.87	0.11	0.06	7.17	0.25	0.021	2.05	99.91	26.19	28.43
80	100	Saka5	49.95	0.70	11.55	3.78	0.012	0.87	0.13	0.05	7.29	0.29	0.030	2.03	99.84	22.83	25.19
100	120	Saka6	52.02	0.67	10.90	3.81	0.011	0.78	0.13	0.05	6.90	0.24	0.020	1.95	99.77	22.61	24.25
120	140	Saka7	48.01	0.65	11.01	4.97	0.012	0.82	0.19	0.05	6.85	0.20	0.022	2.48	99.80	24.96	27.02
140	160	Saka8	55.11	0.75	12.38	4.82	0.018	0.98	0.25	0.06	7.51	0.23	0.019	1.34	99.38	14.63	17.24
160	180	Saka9	48.86	0.64	10.91	4.95	0.033	0.82	1.24	0.06	6.79	1.33	0.020	1.57	99.29	19.71	23.63

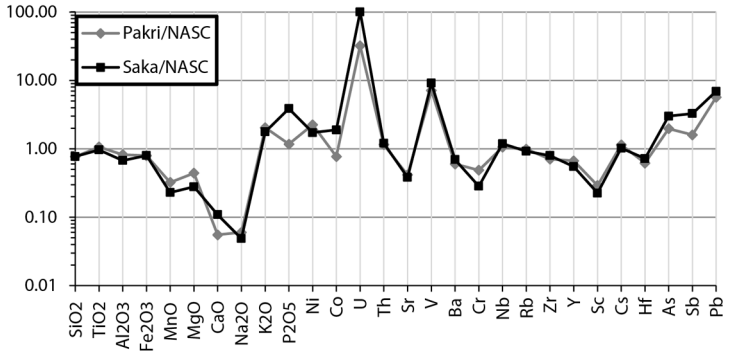

Fig. 3. Major and trace elements of GA samples normalized to NASC (North American Shale Composite) after [40].

black shale complexes. Typically for the organic-rich deposits formed under oxygen deficient environment, the Estonian GA suggests efficient sequestration of sulfur and iron. The content of these elements is, however, highly variable in different samples investigated. The content of Fe_2O_3 in the examined samples varied between 3.79 and 6.08 wt%. The sulfur concentration changed from 1.34 to 4 wt%. The strong correlation between the abundances of sulfur and iron in the Pakri GA sequence indicates that most of the sulfur is incorporated into iron sulfides rather than into organic matter. In the Saka section the correlation between the behaviors of sulfur and iron is less apparent, partly probably due to formation of secondary sulfates and phosphates. P_2O_5 and CaO, whose abundance in GA is generally low, are mainly included in apatite, as suggested by the covariance of those elements in the GA samples. Nevertheless, the detailed variance patterns of phosphorus in Saka and Pakri sequences reveal that on the background of generally monotonous phosphorus content some GA intervals (e.g. Saka2, Saka9, Pakri17) present anomalously high concentrations of P_2O_5. Elevated phosphorus values might be due to the higher level of mixing with phosphatic detritus, suggested by the considerable abundance of phosphatic bioclastic fragments in these GA levels or due to the formation of diagenetic apatite.

If the two GA sequences under study are compared on the basis of major element composition, differences appear to be moderate – the Pakri samples have a slightly higher content of K_2O, Al_2O_3, TiO_2 and MgO and a lower content of CaO and P_2O_5. In general, the relatively homogeneous major element distribution gives limited clues for predicting the highly inhomogeneous trace element enrichment patterns and for unraveling the processes behind enrichment.

4.2. Trace elements

Trace metal enrichment in black shales is mostly explained by two alternative theories: 1) synsedimentary sequestration of metals under oxygen-deficient conditions from marine water, e.g. [41, 12, 20], or 2) flushing of the sediments by metal-enriched syngenetic brines or contemporaneous exhalation of such brines into marine basin, e.g. [42, 14, 43, 25, 30]. However, these theories are challenged by works that underline the influence of source rocks and particulate precursor material on the final character of metal enrichment in black shales, e.g. [44], or the crucial role of diagenetic redistribution processes induced by late diagenetic brines, e.g. [8, 45].

In general, U-Mo-V-Pb enriched trace metal association with sporadically elevated concentrations of some other trace elements was detected in GA from Saka and Pakri sections (Table 2). For assessing the degree of enrichment of particular trace metals in GA, the detected average trace element abundances were compared with average shale and black shale standard compilations. With respect to PAAS and NASC values the GA appears to be extremely enriched in U and V (Fig. 3). For example, the average U concentration in the Saka section (267 ppm) is a hundred times higher than the corresponding values for NASC. There is a nine-fold difference in V concentration between NASC and Saka GA section (average 1190 ppm). If compared with the minimum enrichment values (m.e.v.) for metalliferous black shales (suggested by Vine and Tourtelot [7] on the basis of generalized data of numerous North-American black shales), the studied samples and the Estonian GA in general could be considered enriched with U (m.e.v. 30 ppm), Mo (m.e.v. 200 ppm), V (m.e.v. 1000 ppm), Pb (m.e.v. 100 ppm) and Co (m.e.v. 30 ppm; only in Saka samples) [28].

All previously listed enriched trace metals of GA as well as other abundant trace elements, like As, Sb, Ni, Cu, Re, belong to the group of redox sensitive and/or stable sulfide-forming metals and might undergo considerable partitioning in marine geochemical and biochemical cycles. As indicated by the studies of trace elements in modern marine environments, e.g. [46–48], the redox sensitive elements mostly occur as soluble species under oxidizing conditions. Under the oxygen-depleted conditions, however, the redox sensitive elements are typically present as insoluble species (metal-organic complexes, sulfides, metal oxyhydrates) and thus tend to sequester into sediments. The whole metal trapping process is strongly linked with organic matter breakdown and sulfate reduction processes, which inhibit the crystallization of sulfides. In addition to the redox sensitive trace elements, other elements like Fe and Mn found commonly enriched in black shales, are essential recyclers in redox partitioning in marine systems [49]. Consequently, based on numerous comparative studies of trace element accumulation in modern and ancient organic rich sediments, e.g. [50, 51], it has been suggested that oxygen availability in sedimentary environment could have had sole control over development of enriched trace metal associations in different black shales, e.g. [12].

Table 2. Trace elements in GA samples from Pakri and Saka sections

Interval, cm		Lab	Acme									GI XRF	Acme	GI XRF			Acme	GI XRF					Acme		
			PPM																						
From	To	Sample	Mo	Cu	Pb	Zn	Ni	Co	As	U	Th	Sr	Sb	V	Ba	Cr	Se	Ga	Nb	Rb	Zr	Y	Sc	Be	Li
0	20	Pakri1	639	146	105	45	130	18	55	126	13	62	5.4	1081	398	45	3.7	17.8	13.6	128	129	23	3.3	1.8	17.3
20	40	Pakri2	181	115	75	40	124	16	39	108	12	65	4.3	1166	395	48	3.1	15.6	13.5	127	128	19	3.5	1.6	18.0
40	60	Pakri3	203	134	101	49	166	33	56	206	13	65	5.0	1223	381	51	3.5	15.7	13.0	127	133	19	4.5	2.3	18.8
60	80	Pakri4	148	133	98	845	178	27	51	82	13	63	3.9	1025	384	48	3.3	14.2	12.5	121	134	27	4.5	2.1	16.4
80	100	Pakri5	155	143	116	138	170	24	56	164	14	62	4.2	1061	369	50	3.7	15.0	17.2	125	132	18	5.0	2.3	18.7
100	120	Pakri6	151	133	98	134	144	15	52	172	13	64	4.4	1015	399	54	3.3	15.2	19.5	124	138	17	3.8	2.0	15.3
120	140	Pakri7	157	148	105	42	147	22	55	117	15	63	4.0	1229	347	57	4.1	14.9	15.2	125	136	20	4.8	2.0	17.1
140	160	Pakri8	126	151	193	39	141	21	52	93	15	64	3.3	1144	381	57	4.5	14.0	14.0	126	142	18	4.6	1.3	16.3
160	180	Pakri9	88	162	143	39	115	18	47	78	14	61	2.6	827	374	54	3.1	15.6	14.3	124	131	13	4.4	1.4	15.3
180	200	Pakri10	74	152	135	38	160	22	59	52	14	56	2.5	652	388	71	4.1	14.6	11.9	113	137	24	4.2	1.6	14.5
200	220	Pakri11	61	151	135	60	107	15	72	41	16	57	2.4	563	376	72	3.8	14.5	12.8	117	144	17	4.2	1.3	14.6
220	240	Pakri12	102	129	132	50	115	16	54	91	14	57	3.0	1040	387	65	4.7	12.9	12.6	125	144	21	n.a.	n.a.	n.a.
240	260	Pakri13	110	161	152	40	172	19	68	65	15	55	4.4	1096	318	60	7.7	16.8	13.9	115	139	21	4.7	1.7	15.6
260	280	Pakri14	60	162	174	37	185	21	118	52	14	54	5.2	839	344	62	5.8	12.5	10.7	105	140	31	4.2	2.0	14.6
280	300	Pakri15	92	131	103	40	133	21	52	76	14	59	3.1	1081	408	57	4.3	15.0	14.0	128	140	21	4.5	1.2	16.1
300	320	Pakri16	85	144	117	42	120	17	54	102	15	56	3.5	1096	358	63	4.0	16.2	15.9	128	138	13	4.6	1.0	15.4
320	340	Pakri17	96	120	105	38	113	35	63	82	16	67	3.3	739	377	48	3.7	13.9	10.6	118	148	73	5.0	1.3	14.9
340	360	Pakri18	53	141	103	41	96	17	45	35	14	54	2.2	781	377	70	2.9	16.7	13.2	131	142	21	4.9	1.2	16.7
360	380	Pakri19	57	129	100	42	104	15	53	49	16	54	2.7	925	429	73	4.8	16.5	12.7	128	150	23	4.7	1.0	16.4
380	400	Pakri20	52	125	94	40	116	17	55	19	14	48	2.0	622	393	56	2.6	15.9	12.3	121	153	21	4.1	1.0	14.6
400	420	Pakri21	65	101	88	36	99	17	65	57	14	55	2.1	745	369	74	3.6	13.7	13.4	119	157	40	n.a.	n.a.	n.a.
0	20	Saka1	1143	76	193	14	82	44	64	137	13	62	9.1	1266	390	36	5.3	15.0	16.0	120	168	9	2.8	0.5	3.9
20	40	Saka2	85	85	187	10	103	102	76	182	16	56	5.3	946	409	36	5.7	12.0	10.0	92	171	31	3.6	0.6	3.1

Table 2 (continuation)

Interval, cm		Lab	Acme									GI XRF	Acme	GI XRF			Acme	GI XRF					Acme		
			PPM																						
From	To	Sample	Mo	Cu	Pb	Zn	Ni	Co	As	U	Th	Sr	Sb	V	Ba	Cr	Se	Ga	Nb	Rb	Zr	Y	Sc	Be	Li
40	60	Saka3	97	134	152	14	82	62	86	169	15	52	4.5	1093	406	32	5.3	16.0	17.0	108	155	12	3.2	0.8	4.1
60	80	Saka4	1844	176	101	25	89	31	72	805	16	51	9.9	1497	438	41	5.5	16.0	19.0	141	165	6	4.8	1.2	9.1
80	100	Saka5	202	122	135	22	89	43	54	111	16	49	5.5	1453	435	38	5.1	15.0	14.0	116	163	11	3.1	0.7	7.1
100	120	Saka6	408	106	124	21	88	25	57	433	14	47	5.7	1288	441	30	4.3	13.0	16.0	122	160	9	3.0	0.7	6.9
120	140	Saka7	413	108	137	36	127	28	50	239	14	50	7.2	1165	390	31	4.1	13.0	21.0	114	135	16	2.7	0.5	8.1
140	160	Saka8	279	116	125	116	118	51	75	145	16	56	6.5	1096	421	38	5.6	11.0	16.0	121	173	23	3.8	0.9	9.8
160	180	Saka9	299	148	95	23	125	53	236	184	15	66	8.0	908	650	38	7.1	10.0	10.0	102	149	57	3.2	0.8	7.8

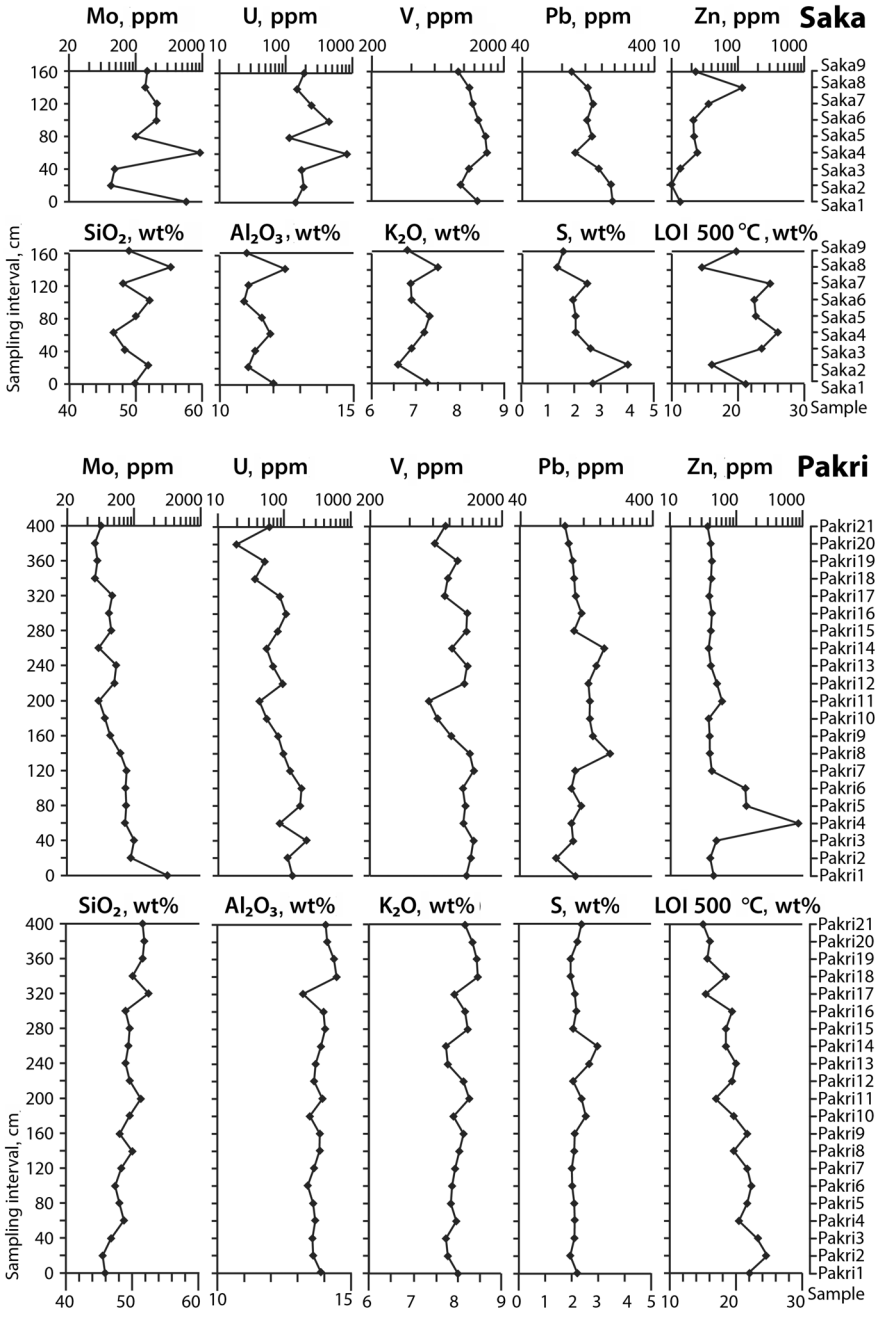

Fig. 4. Vertical distribution profiles of major compounds SiO_2, Al_2O_3, K_2O, S, and LOI 500 °C and enriched trace metals from Saka and Pakri GA sections.

The performed geochemical investigations revealed that the studied sequences present pronounced vertical variations in U, V, Mo and Zn con-

centrations (Fig. 4). The listed trace elements do not show completely matching variance patterns and the maximum (and minimum) enrichment intervals of different components mostly do not overlap. In case of the Pakri GA sequence one can separate about 1.3 m thick lower part, which is enriched with some trace metals like Mo, U and Sb, and also contains more organic matter as indicated by higher LOI 500 °C values. While Mo is gradually decreasing towards the upper part of the Pakri sequence, U and V contents are somewhat more erratic. The thinner GA complex from Saka, which on average contains more Mo, U and V than the Pakri GA, is also characterized by the larger variance of those elements. In Saka samples, no clear vertical distribution trends of Mo and U can be followed, the concentrations fluctuate on a large scale and very high values alternate with low ones. For example, in samples Saka1 and Saka4 the Mo content is 1143 and 1843 ppm, respectively, while between these samples it only varies between 85 and 97 ppm. In general, Mo and U contents in the Saka section show quite a strong positive covariance with organic matter content (LOI 500 °C). The sample Saka4, which presents anomalously high values of these elements, also yielded the highest LOI 500 °C value. These results agree with the observation that the contents of V, U and Mo in black shales typically correlate with the abundance of organic matter [7], likely indicating early fixation via metal-organic complexes. However, in case of V, which shows considerably high values throughout both studied GA sequences, the correlation with organic matter is less expressed.

The average content of Pb is similar in both investigated sections and its vertical distribution is rather homogeneous. Lead shows a positive covariance with elements presumably related with sulfides – Fe_2O_3, S, Cu, Se, Ag, Hg in Pakri samples, while in Saka there is a positive correlation with S and Ta, and a negative one with Cu, Li, Re, Sn. Zn generally demonstrates an opposite trend to internally enriched elements such as U, V, Mo. Its abundance is two times higher in Pakri samples compared to Saka ones. However, the elevated concentrations of Zn in the Pakri section (up to 761 ppm in Pakri4) are limited to the well-defined interval 60–120 cm from the bottom, whereas the rest of the sequence is characterized by a monotonous Zn concentration near 40–60 ppm. In the Saka section the content of Zn is very low in the lower part of the section, but shows a general increase toward the upper part of the complex. The pronounced positive covariance of Cd with Zn in the studied sequences likely indicates a coeval trapping of those phases during sphalerite formation.

U positive covariance with P_2O_5 was not detected in the samples under study. Trace metal partitioning into phosphates has been suggested by some studies [52] as a process responsible for the higher general concentration of U in the GA of NE Estonia.

In general, the dominance of common marine redox sensitive elements among enriched metals in GA favors syngenetic enrichment as the major process of trace metal sequestration. On the other hand, the remarkably high

concentration of enriched elements in GA and the variable covariance patterns imply that element sequestration solely from seawater due to Eh gradients is likely an insufficient model for explaining the observed large-scale trace metal heterogeneity in GA. Furthermore, the current data (Tables 2, 3) as well as previous studies [2] indicate that besides the elements, for which partitioning in marine systems is well known, GA sporadically presents elevated levels of some minor elements, e.g. PGE and W, characterized by generally very low abundance in average crust and modern marine sediments. The accumulation of such minor compounds in GA underlines the role of internal input of metals into the sedimentary or diagenetic environment.

The closeness of probable denudation areas (the peneplain of Proterozoic crystalline rocks in Southern Finland) to the sedimentary setting where GA accumulated hints that the trace elemental composition of sea water in these areas likely bore a distinct terrestrial signature, similarly to recent coastal marine environments [49]. Moreover, recent studies in Caledonian Nappe complexes, e.g. [53], suggest the existence of subduction zone related volcanic arc complexes within the Iapetus Ocean near the western border of the Baltica paleocontinent in the Late Cambrian and Tremadoc. The associated volcanic activity in these areas could supply overlying waters with extra trace metal budgets and modify regional marine trace metal signals enhancing, for example, Zn and V content of marine water. Then again, the likely introduction of the particulate volcanic matter to the sedimentary basin during the times of GA formation is suggested by clay mineral studies. According to Utsal et al. [35] the widespread occurrence of authigenic illite-smectite in GA indicates that at least 10% of its primary sedimentary matter was made up of volcanic ash.

The differences in trace element composition of GA might thus in some instances reflect variations in source material fluxes. First of all this relates to non-reactive elements with negligible solubility in surface environments transported to the sedimentary basin mainly in the composition of terrigenic (volcanic) matter such as residual heavy minerals, secondary weathering products or volcanic ash. According to Vine and Tourtelot [7], the detrital fraction of most black shales is characterized by the elements Al, Ti, Zr, Ga, Sc, and may also commonly include Be, B, Ba, Na, K, Mg, and Fe. Additional elements generally considered insensitive to secondary processes include Nb, Y, Th, Ta, Hf, and the REEs [39].

On the La-Al and La-Ti diagrams (Figs. 5A, 5B) the distribution of Al and Ti shows a similar pattern with respect to the lanthanum behavior. The Pakri samples with higher alumina and silica values and somewhat higher Ti content have enhanced La values as compared to Saka samples. The covariance of La with typical detrital compounds suggests that La may be dominantly bounded by detrital phases. However, the abnormally high La content detected in three phosphorus-rich samples may suggest a possible synsedimentary incorporation into the biogenic detritus or diagenetic

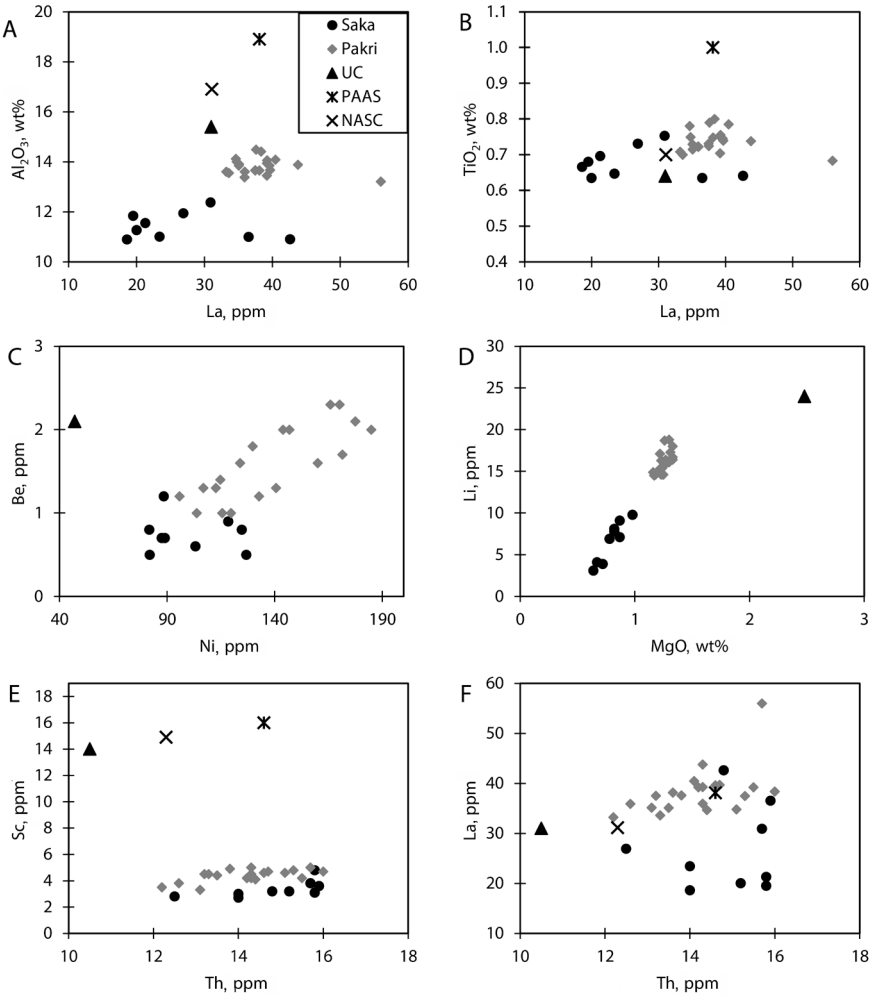

Fig. 5. Relationships between trace elements in graptolite argillite. UC = Upper Continental Crust [55]; PAAS = Post Archaean Australian Shale [39]; NASC = North American Shale Composite [40].

mobility of La. Be and Ni abundances in the Pakri section demonstrate a two-line positive covariance trend (Fig. 5C). Such a distribution pattern of two elements with generally different geochemical behavior in surface systems might reflect the terrigenic (volcanogenic) flux into the sedimentary environment from a distinct source during the initial period of accumulation of the GA or specific sedimentary conditions supporting Ni enrichment. The terrigenic flux controlled abundance is suggested also for Li and Mg (Fig. 5D). Both elements show a very well defined positive correlation, suggesting that Li and Mg are likely bonded into the crystal structure of micas and/or clay minerals. Figures 5E and 5F present the relations of Sc, Th,

and La, widely exploited for discriminating different magmatic rock types and settings. Numbers of studies have employed these variations to track possible precursor rocks of ancient shale and black shale complexes [39, 54]. On the Th-Sc graph the Pakri and Saka samples present anomalously low Sc and high Th/Sc content (Fig. 5E), thus suggesting a generally felsic upper crustal precursor for GA. The La/Th ratios of the analyzed GA samples demonstrate considerably higher scattering. As mentioned above, however, the enhanced La values in phosphorus-rich samples suggest that precursor rock signal had been in some cases evidently obscured by the synsedimentary incorporation or posterior redistribution of La.

In general, the clustering of non-reactive trace element data into the two fields may suggest that two different dominant source areas were involved in the supply of detrital material to the localities where organic-rich muds once accumulated.

4.3. Rare earth element variations

The REE patterns recorded for post-Archaean shales (PAAS) show striking similarity worldwide: they are light REE enriched, with a negative Eu anomaly and relatively flat heavy REEs [55, 39]. Samples from Pakri show chondrite-normalized (CN) REE patterns (Fig. 6C) generally similar to those recorded for PAAS, being considerably enriched in light rare earth elements (LREEs) with respect to heavy rare earth elements (HREEs). The main difference from the average shale compilations appears in content of MREEs (Fig. 6B). Like PAAS, all the studied samples exhibit negative Eu anomaly. The La_{CN}/Yb_{CN} ratio ranges from 6.65 to 10.26, staying thus well below the upper crust's La_{CN}/Yb_{CN} ratio. The Gd_{CN}/Yb_{CN} ratio varies from 1.09 to 2.22 with an average of 1.44 which is close to the PAAS value. The PAAS-normalized REE patterns of the examined GA samples show generally flat shape (Figs. 6A, 6B). In respect of the considerably monotonous REE variations, three samples from the Pakri locality exhibit distinct behavior. Pakri21 and Pakri14 have similar REE fractionation patterns with a somewhat elevated content of MREEs compared to PAAS. A unique hat-shape REE shale-normalized pattern was recorded for Pakri17 sample, which also presents a clearly elevated absolute REE concentration and strong MREEs enrichment. Compared to the Pakri sequence the REE patterns for Saka samples show higher fractionation and variation in the content of REEs (Figs. 6A, 6C). The La_{CN}/Yb_{CN} ratio is similar to that in Pakri samples, except in Saka1 and Saka4 where it reaches 15.56 and 14.27, respectively. The Gd_{CN}/Yb_{CN} ratios show high variation from 0.66 to 2.76, being the highest in samples Saka2 and Saka3. The MREE pattern shows higher variation than in Pakri samples. The PAAS-normalized REE patterns of Saka1, Saka4, Saka5, and Saka6 show low REE absolute abundances, but are characterized by distinctive concave shape patterns with considerably enriched HREEs (Tm-Yb) with respect to depleted MREEs (Ce-Er). Remarkably, these samples have the lowest content of Fe_2O_3 and the highest

contents of Mo, U and V (though high contents of these trace elements also occur in other samples). The hat-shaped (similar to that of Pakri17), MREE enriched patterns characterize Saka2 and Saka3 samples. The REE patterns of samples Saka7, Saka8, and Saka9 are more flat-shaped, similar to a typical Pakri pattern.

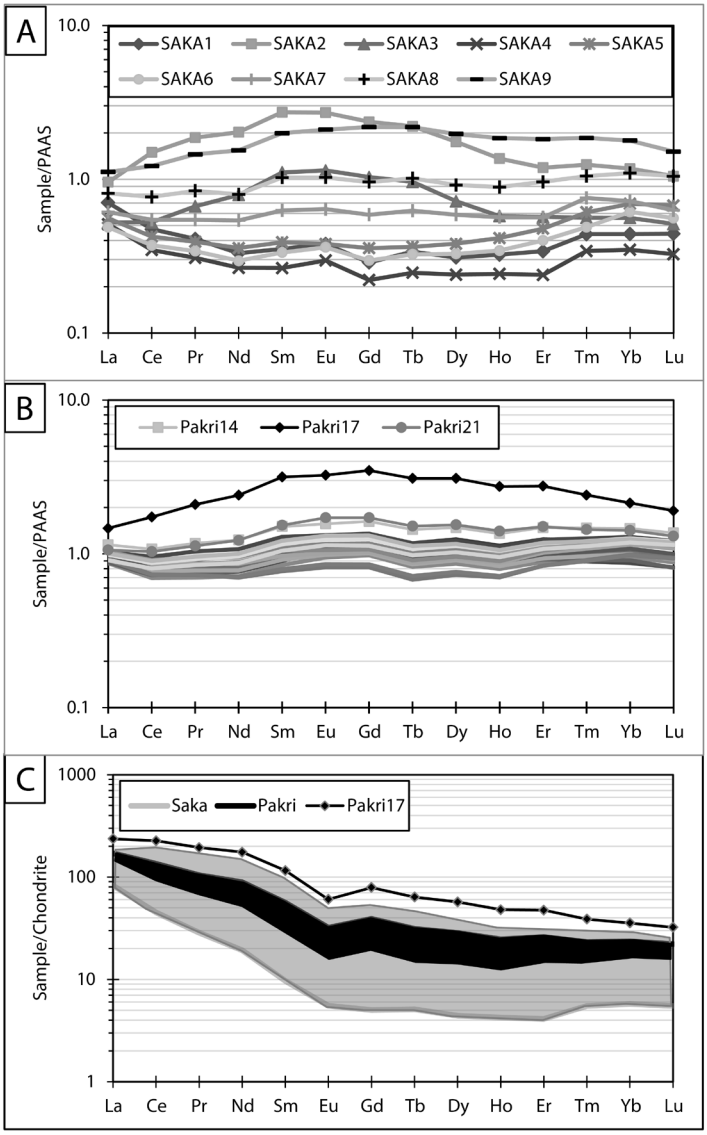

Fig. 6. Rare earth element patterns of GA samples normalized to PAAS (A; B) [39] and chondrite (C).

Table 3. Rare earth elements in GA samples from Pakri and Saka sections, ppm

Lab	Sample	La	Ce	Pr	Nd	Sm	Eu	Gd	Tb	Dy	Ho	Er	Tm	Yb	Lu
GI; Acme	Pakri1	35.1	58.5	6.5	26.0	5.0	1.14	5.07	0.70	4.22	0.83	2.51	0.37	2.46	0.35
GI; Acme	Pakri2	33.2	55.4	6.2	24.2	4.7	1.02	4.56	0.63	4.03	0.79	2.53	0.37	2.67	0.38
GI	Pakri3	33.6	57.7	6.6	26.1	5.3	1.12	4.92	0.70	4.43	0.85	2.63	0.37	2.56	0.35
GI	Pakri4	37.5	68.6	8.1	32.5	6.6	1.38	6.28	0.90	5.81	1.12	3.54	0.50	3.48	0.49
GI	Pakri5	35.9	62.4	7.2	28.1	5.6	1.16	5.11	0.72	4.62	0.89	2.85	0.42	2.90	0.41
GI; Acme	Pakri6	35.9	61.0	6.9	26.5	5.1	1.07	4.70	0.66	4.25	0.82	2.66	0.40	2.81	0.40
GI	Pakri7	37.5	65.8	7.6	29.6	5.8	1.17	5.09	0.72	4.54	0.88	2.83	0.42	3.05	0.43
GI	Pakri8	39.6	68.1	7.6	29.2	5.5	1.09	4.80	0.67	4.36	0.87	2.90	0.44	3.24	0.46
GI	Pakri9	35.1	58.5	6.4	23.8	4.3	0.88	3.81	0.52	3.42	0.70	2.38	0.37	2.79	0.41
GI	Pakri10	39.2	76.0	9.1	36.4	7.2	1.43	6.30	0.90	5.67	1.10	3.51	0.52	3.63	0.52
GI	Pakri11	39.2	72.4	8.3	31.5	5.9	1.14	4.98	0.70	4.49	0.89	2.99	0.46	3.40	0.50
GI; Acme	Pakri12	38.1	70.0	8.2	31.9	6.2	1.23	5.41	0.77	4.93	0.96	3.15	0.47	3.37	0.49
GI	Pakri13	39.7	71.8	8.3	32.3	6.2	1.25	5.45	0.78	5.00	0.98	3.21	0.49	3.48	0.50
GI	Pakri14	43.8	85.4	10.3	41.7	8.4	1.69	7.57	1.11	6.93	1.34	4.22	0.60	4.12	0.59
GI	Pakri15	39.2	72.0	8.4	33.2	6.6	1.36	5.91	0.84	5.28	1.01	3.23	0.48	3.40	0.48
GI	Pakri16	34.8	58.0	6.4	24.1	4.5	0.93	3.99	0.55	3.57	0.71	2.39	0.37	2.76	0.40
GI	Pakri17	56.0	138.2	18.4	81.6	17.7	3.51	16.23	2.38	14.48	2.71	7.86	0.99	6.04	0.82
GI	Pakri18	37.6	69.3	8.1	32.6	6.5	1.35	5.83	0.83	5.26	1.03	3.33	0.50	3.55	0.52
GI	Pakri19	38.4	71.6	8.4	33.9	6.8	1.42	6.13	0.87	5.44	1.05	3.36	0.49	3.51	0.51
GI	Pakri20	34.6	63.9	7.4	29.5	5.9	1.23	5.25	0.75	4.78	0.94	3.07	0.46	3.34	0.49
GI; Acme	Pakri21	40.4	82.3	9.9	41.5	8.6	1.86	8.01	1.17	7.23	1.39	4.29	0.59	4.01	0.56
Acme	Saka1	26.9	37.7	3.6	11.2	2.0	0.41	1.34	0.26	1.45	0.32	0.97	0.18	1.24	0.19
Acme	Saka2	36.5	119.0	16.4	68.6	15.3	2.93	11.00	1.70	8.19	1.35	3.39	0.51	3.30	0.45
Acme	Saka3	20.0	41.7	5.9	26.8	6.2	1.23	4.81	0.74	3.37	0.57	1.62	0.23	1.58	0.22
Acme	Saka4	19.5	27.6	2.7	9.0	1.5	0.32	1.03	0.19	1.12	0.24	0.68	0.14	0.98	0.14
Acme	Saka5	21.3	33.7	3.5	12.1	2.2	0.41	1.66	0.28	1.78	0.41	1.36	0.25	1.95	0.29
Acme	Saka6	18.6	29.6	3.0	10.0	1.9	0.39	1.38	0.25	1.53	0.34	1.14	0.20	1.73	0.24
Acme	Saka7	23.4	43.4	4.8	18.3	3.5	0.69	2.74	0.48	2.75	0.56	1.61	0.31	2.03	0.27
Acme	Saka8	30.9	61.1	7.4	27.0	5.7	1.11	4.47	0.78	4.29	0.88	2.74	0.43	3.09	0.45
Acme	Saka9	42.6	97.0	12.8	52.2	11.2	2.27	10.17	1.68	9.21	1.83	5.20	0.76	5.03	0.65

The observed large-scale variations in REE patterns – the encounter of normal flat shape as well as hat and concave like patterns – could be explained by variations in detrital input, e.g. variations in accessory mineral associations. However, alternatively it might point to the possibility that in most samples of the Saka sequence and in some intervals of Pakri the source rock inherited REE signals have been masked or obscured by the synsedimentary, diagenetic, hydrothermal or weathering induced redistribution-enrichment of REEs. The recent studies of black shales have indicated that authigenic phases such as sulfides, phosphates and carbonates as well as organic matter may host elevated REEs and their presence might influence

the absolute abundances of REEs as well as the fractionation patterns, e.g. [56]. Cruse et al. [57] interpreted the intermittent occurrence of hat and concave shape shale-normalized REE patterns in authigenic phosphate-rich and low-phosphate black shales as the evidence of an early diagenetic redistribution of REEs formed as the result of a preferential uptake of MREE in apatite and simultaneous depletion of phosphate-poor host shale beds. A similar enrichment process could be hypothesized for the MREE enriched samples of Saka and Pakri GA, all characterized by elevated phosphorus content compared to the rest of the samples under study. This agrees with high REE values detected by SEM analysis of authigenic as well as bioclastic phosphates in the studied sequences. Lev et al. [58] demonstrated the importance of post-/syn-depositional mineralizing fluid induced disturbance in REE-systems together with redistribution of U in black shales. Consequently, the encountered REE fractionation patterns could theoretically indicate also the influence of short-term low temperature brines. In case of GA the possible influence of deep source brines on the formation of its mineral assemblage has been suggested previously by sulfur isotope studies of pyrite [25]. However, the influence of deep brines on the Estonian Lower Paleozoic sedimentary assemblage is problematic as the whole complex is thermally almost unaltered. On the other hand, Somelar et al. (2010) [59] suggested intrusion of low temperature K-rich brines as the mechanism behind the illitization of Estonian Ordovician K-bentonites, pointing to the possible wide-scale influence of alkaline brines on the region in the Late Silurian.

Nevertheless, despite the lack of knowledge of the precise formation mechanism of the observed variability of REEs, it might suggest REE mobility in sedimentary or diagenetic environments. One could also speculate that the co-appearance of MREE depleted patterns and enhanced U, V and Mo abundances in GA from the Saka outcrop might indicate that those enriched elements were affected by the same redistribution processes which resulted in the formation of MREE depleted patterns.

5. Conclusions

The studies of two vertical sequences of graptolite argillite (GA) show the existence of pronounced fine-scale trace metal variability in GA. The examined samples were detected to be enriched in U, V, Mo and Pb with respect to average black shales, the obtained results thus agreeing with previously published data on the geochemistry of GA. The content of enriched elements was, however, recorded to change greatly over the examined sequences, suggesting a notably more complex nature of trace metal distribution in GA than previously assumed. Redox sensitive metals U and Mo, and also V to a lesser extent, showed loose covariance with organic matter content (LOI 500 °C), apparently indicating their trapping mainly via

organic matter tied species, and the enrichment primary linked to organic matter sequestration. The elevated abundance of a number of other trace metals, e.g. Pb, Zn, Cd, Cu, As and La, was detected in samples with an enhanced content of sulfur or phosphorus. The remarkably different behavior of the listed elements in two examined GA sequences could suggest that somewhat different sets of metal sequestration driving processes were responsible for the development of trace elemental assemblages in E and NW Estonian settings. As the trace element composition of GA is dominated by common marine redox sensitive and/or stable sulfide forming metals, the syngenetic trapping of metals from sea and interstitial water in redox boundary zones probably had first rate control over the development of trace element enrichment patterns. However, the observed high variability in the trace metal composition of GA, including heterogeneous REE patterns, points to the polygenetic nature of metal assemblages, apparently formed as the cumulative product of multistage evolution. On the whole, the study demonstrates that the knowledge base about metal distribution in GA is still rather fragmentary and that detailed geochemical, as well as multi-disciplinary investigations are essential for adequately predicting potential metal resources of GA in the future.

Acknowledgements

The authors are thankful to the reviewers for their constructive criticism and for helping to improve the manuscript. This study was funded by the Estonian Science Foundation Grant No. 8963 and the Estonian Ministry of Education and Research target research project No. SF0140016s09.

REFERENCES

1. Heinsalu, H., Viira, V. Pakerort Stage. In: *Geology and Mineral Resources of Estonia* (Raukas, A., Teedumäe, A., eds.). Estonian Academy Publishers, Tallinn, 1997, 52–58.
2. Petersell, V. Dictyonema argillite. In: *Geology and Mineral Resources of Estonia* (Raukas, A., Teedumäe, A., eds.). Estonian Academy Publishers, Tallinn, 1997, 313–326.
3. Andersson, A., Dahlman, B., Gee, D. G., Snäll, S. The Scandinavian Alum Shales. *Sveriges Geologiska Undersökning* (*SGU*), 1985, **56**, 1–50.
4. Kaljo, D., Borovko, N., Heinsalu, H., Khazanovich, K., Mens, K., Popov, L., Sergeeva, S., Sobolevskaya, R., Viira, V. The Cambrian-Ordovician boundary in the Baltic-Ladoga clint area (North Estonia and Leningrad Region, USSR). *Proc. Acad. Sci. Estonian SSR, Geology*, 1986, **35**(3), 97–108.
5. Heinsalu, H., Bednarczyk, W. Tremadoc of the East European Platform: Lithofacies and palaeogeography. *Proc. Est. Acad. Sci. Geol*., 1997, **46**(2), 59–74.

6. Buchardt, B., Nielsen, A. T., Schovsbo, N. H. Alum shale in Scandinavia (Alun skiferen i Skandinavien). *Geologisk Tidsskrift*, 1997, 3, 1–30 (in Danish).
7. Vine, J. D., Tourtelot, E. B. Geochemistry of black shale deposits – a summary report. *Econ. Geol*., 1970, **65**, 253–272.
8. Coveney, R. M. Jr., Leventhal, J. S., Glascock, M. D., Hatch, J. R. Origins of metals and organic matter in the Mecca Quarry Shale Member and stratigraphically equivalent beds across the Midwest. *Econ. Geol*., 1987, **82**, 915–933.
9. Quinby-Hunt, M. S., Wilde, P., Orth, C. J., Berry, W. B. N. Elemental geochemistry of black shales – statistical comparison of low-calcic shales with other shales. In: *Metalliferous Black Shales and Related Ore Deposits* (Grauch, R. I., Leventhal, J. S., eds.), US Geological Survey Circular, 1989, No. **1037**, 8–15.
10. Wilde, P., Quinby-Hunt, M. S., Berry, W. B. N., Orth, C. J. Palaeo-oceanography and biogeography in the Tremadoc (Ordovician) Iapetus Ocean and the origin of the chemostratigraphy of *Dictyonema flabelliforme* black shales. *Geol. Mag*., 1989, **126**(1), 19–27.
11. Hatch, J. R., Leventhal, J. S. Relationship between inferred redox potential of the depositional environment and geochemistry of the Upper Pennsylvanian (Missourian) Stark Shale Member of the Dennis Limestone, Wabaunsee County, Kansas, U.S.A. *Chem. Geol*., 1992, **99**(1–3), 65–82.
12. Algeo, T. J., Maynard, J. B. Trace-element behavior and redox facies in core shales of Upper Pennsylvanian Kansas-type cyclothems. *Chem. Geol*., 2004, **206**, 289–318.
13. Steiner, M., Wallis, E., Erdtmann, B.-D., Zhao, Y. L., Yang, R. D. Submarine-hydrothermal exhalative ore layers in black shales from South China and associated fossils – insights into a Lower Cambrian facies and bio-evolution. *Palaeogeogr. Palaeocl*., 2001, **169**(3–4), 165–191.
14. Jiang, S. Y., Yang, J. H., Ling, H. F., Chen, Y. Q., Feng, H. Z., Zhao, K. D, Ni, P. Extreme enrichment of polymetallic Ni- Mo-PGE-Au in Lower Cambrian black shales of South China: an Os isotope and PGE geochemical investigation. *Palaeogeogr. Palaeocl*., 2007, **254**(1–2), 217–228.
15. Vaughan, D. J., Sweeney, M., Diedel, G. F. R., Haranczyk, C. The Kupferschiefer: An overview with an appraisal of the different types of mineralization. *Econ. Geol*., 1989, **84**, 1003–1027.
16. Sundblad, K., Gee, D. G. Occurrence of a uraniferous-vanadiniferous graphitic phyllite in the Köli Nappes of the Stekenjokk area, central Swedish Caledonides. *Geol. Foren. Stock. For*., 1984, **106**(3), 269–274.
17. Berry, W. B. N., Wilde, P., Quinby-Hunt, M. S., Orth, C. J. Trace element signatures in Dictyonema shales and their geochemical and stratigraphic significance. *Norsk Geol. Tidsskr*., 1986, **66**, 45–51.
18. Leventhal, J. S. Comparative geochemistry of metals and rare earth elements from the Cambrian alum shale and kolm of Sweden. *Sp. Publ. Int*., 1990, **11**, 203–215.
19. Leventhal, J. S. Comparison of organic geochemistry and metal enrichment in two black shales: Cambrian Alum Shale of Sweden and Devonian Chattanooga Shale of United States. *Miner. Deposita*, 1991, **26**, 104–112.
20. Schovsbo, N. H. Uranium enrichment shorewards in black shales: A case study from the Scandinavian Alum Shale. *Geol. Foren. Stock. For*., 2002, **124**(2), 107–115.

21. Loog, A. Geochemistry of Lower Ordovician of Estonia. In: *Studies of the Institute of Geology, ESSR Academy of Sciences*. Tallinn, 1962. No. 10, 273–291 (in Russian).
22. Baukov, S. S. General characteristics of dictyonema shale. In: *Geology of Coal and Oil Shale Deposits of the USSR*, **11**. Nedra, Moscow, 1968, 145–148 (in Russian).
23. Petersell, V., Mineyev, D., Loog, A. Mineralogy and geochemistry of obolus sandstones and dictyonema shale of North Estonia. *Acta et Commentationes Universitatis Tartuensis*, No. 561, Tartu, 1981, 30–49 (in Russian).
24. Loog, A. On the geochemistry of postsedimentary mineral formation in the Tremadoc graptolitic argillites of North Estonia. *Acta et Commentationes Universitatis Tartuensis*, No. 527, Tartu, 1982, 44–49 (in Russian).
25. Petersell, V. H., Zhukov, F. I., Loog, A. R., Fomin, Y. A. Origin of Tremadoc kerogenous-bearing siltstones and argillites of North Estonia. *Oil Shale*, 1987, **4**(1), 8–13 (in Russian).
26. Pukkonen, E. M. Major and minor elements in Estonian graptolite argillite. *Oil Shale*, 1989, **6**(1), 11–18 (in Russian).
27. Kallaste, T., Pukkonen, E. Pyrite varieties in Estonian Tremadocian argillite (Dictyonema shale). *Proc. Est. Acad. Sci. Geol*., 1992, **41**(1), 11–22.
28. Pukkonen, E., Rammo, M. Distribution of molybdenum and uranium in the Tremadoc graptolitic argillite (Dictyonema shale) of North-Western Estonia. *Bulletin of the Geological Survey of Estonia*, 1992, **2**(1), 3–15.
29. Loog, A., Petersell, V. The distribution of microelements in Tremadoc graptolitic argillite of Estonia. *Acta et Commentationes Universitatis Tartuensis*, No. 972, Tartu, 1994, 57–75.
30. Loog, A., Petersell, V. Authigenic siliceous minerals in the Tremadoc graptolitic argillite of Estonia. *Proc. Est. Acad. Sci. Geol*., 1995, **44**(1), 26–32.
31. Heinsalu, H. Lithostratigraphical subdivision of Tremadoc deposits of North Estonia. *Proc. Acad. Sci. Estonian SSR, Geology*, 1987, **36**(2), 66–78 (in Russian).
32. Raudsep, R. Ordovician. Pakerort Stage. Ceratopyge Stage. In: *Geology and mineral resources of the Rakvere phosphorite-bearing area* (Puura, V., ed.). Valgus, Tallinn, 1987, 29–39 (in Russian).
33. Kaljo, D., Kivimägi, E. On the distribution of graptolites in the Dictyonema shale of Estonia and the noncontemporaneity of its different facies. *Proc. Acad. Sci. Estonian SSR, Chem., Geol*., 1970, **19**(4), 334–341 (in Russian).
34. Kiipli, T., Batchelor, R. A., Bernal, J. P., Cowing, C., Hagel-Brunnström, M., Ingham, M. N., Johnson, D., Kivisilla, J., Knaack, C., Kump, P., Lozano, R., Michiels, D., Orlova, K., Pirrus, E., Rousseau, R. M., Ruzicka, J., Sandström, H., Willis, J. P. Seven sedimentary rock reference samples from Estonia. *Oil Shale*, 2000, **17**(3), 215–223.
35. Utsal, K., Kivimägi, E., Utsal, V. About the method of investigating Estonian graptolitic argillite and its mineralogy. *Acta et Commentationes Universitatis Tartuensis*, No. 527, Tartu, 1982, 116–136 (in Russian).
36. Loog, A., Kurvits, T., Aruväli, J., Petersell, V. Grain size analysis and mineralogy of the Tremadocian Dictyonema shale in Estonia. *Oil Shale*, 2001, **18**(4), 281–297.
37. Kleesment, A.-L., Kurvits, T. U. Mineralogy of Tremadoc graptolitic argillites of North Estonia. *Oil Shale*, 1987, **4**(2), 130–138 (in Russian).

38. Snäll, S. Mineralogy and maturity of the alum shales of south-central Jämtland, Sweden. *Sveriges Geologiska Undersökning* (*SGU*), 1988, Serie C, **818**, 1–46.
39. Taylor, S. R., McLennan, S. M. *The Continental Crust: its Composition and Evolution*. Blackwell Scientific Publication, Oxford, 1985.
40. Gromet, L. P., Dymek, R. F., Haskin, L. A., Korotev, R. L. The "North American shale composite": its compilation, major and trace element characteristics. *Geochim. Cosmochim. Ac*., 1984, **48**, 2469–2482.
41. Holland, H. D. Metals in black shales – A reassessment. *Econ. Geol*., 1979, **74**, 1676–1680.
42. Coveney, R. M. Jr., Glascock, M. D. A review of the origins of metal-rich Pennsylvanian black shales, central U.S.A., with an inferred role for basinal brines. *Appl. Geochem*., 1989, **4**(4), 347–367.
43. Yu, B., Dong, H., Widom, E., Chen, J., Lin, C. Geochemistry of basal Cambrian black shales and cherts from the Northern Tarim Basin, Northwest China: Implications for depositional setting and tectonic history. *J. Asian Earth Sci*., 2009, **34**(3), 418–436.
44. Leventhal, J. S., Hosterman, J. W. Chemical and mineralogical analysis of Devonian black-shale samples from Martin County, Kentucky; Carroll and Washington counties, Ohio; Wise County, Virginia; and Overton County, Tennessee, U.S.A. *Chem. Geol*., 1982, **37**(3–4), 239–264.
45. Peacor, D. R., Coveney, R. M. Jr., Zhao, G. Authigenic illite and organic matter: the principal hosts of vanadium in the Mecca Quarry shale at Velpen, Indiana. *Clay. Clay Miner*., 2000, **48**(3), 311–316.
46. Calvert, S. E., Pedersen, T. F. Geochemistry of recent oxic and anoxic marine sediments: Implications for the geological record. *Mar. Geol*., 1993, **113**(1–2), 67–88.
47. Nameroff, T. J., Balistrieri, L. S., Murray, J. W. Suboxic trace metal geochemistry in the Eastern Tropical North Pacific. *Geochim. Cosmochim. Ac*., 2002, **66**(7), 1139–1158.
48. Morford, J. L., Emerson, S. The geochemistry of redox sensitive trace metals in sediments. *Geochim. Cosmochim. Ac*., 1999, **63**(11–12), 1735–1750.
49. Chester, R. *Marine Geochemistry*. Blackwell, London, 2000.
50. Nijenhuis, I. A., Bosch, H.-J., Sinninghe Damsté, J. S., Brumsack, H.-J., De Lange, G. J. Organic matter and trace element rich sapropels and black shales: a geochemical comparison. *Earth Planet. Sc. Lett*., 1999, **169**(3–4), 277–290.
51. Brumsack, H.-J. The trace metal content of recent organic carbon-rich sediments: implications for Cretaceous black shale formation. *Palaeogeogr. Palaeocl*., 2006, **232**(2–4), 344–361.
52. Kochenov, A. V., Baturin, G. N. The paragenesis of organic matter, phosphorus and uranium in marine sediments. *Lithology and Mineral Resources*, 2002, **37**(2), 107–120.
53. Grimmer, J. C., Greiling, R. O. Serpentinites and low-K island arc metavolcanic rocks in the Lower Köli Nappe of the central Scandinavian Caledonides: Late Cambrian – early Ordovician serpentinite mud volcanoes in a forearc basin? *Tectonophysics*, 2012, **541–543**, 19–30.
54. Quinby-Hunt, M. S., Wilde, P., Orth, C. J.,Berry, W. B. N. The provenance of low-calcic black shales. *Miner. Deposita*, 1991, **26**(2), 113–121.

55. Rudnick R. L., Gao, S. Composition of the continental crust. In: *Readings from the Treatise on Geochemistry* (Holland, H. D., Turekian, K. K., eds.). Elsevier, Amsterdam, 2010, 131–198.
56. Lev, S. M., McLennan, S. M., Hanson, G. N. Mineralogic controls on REE mobility during black-shale diagenesis. *J. Sediment. Res*., 1999. Vol. 69. P. 1071–1082.
57. Cruse, A. M., Lyons, T. W., Kidder, D. L. Rare-earth element behavior in phosphates and organic-rich host shales: An example from the Upper Carboniferous of Midcontinent North America. In: *Marine Authigenesis: From Global to Microbial* (Glenn, C. R., Prévôt-Lucas, L., Lucas, J., eds.), SEPM Special Publication, 2000, **66**, 445–453.
58. Lev, S. M., Filer, J. K., Tomascak, P. Orogenesis vs. Diagenesis: Can we use organic-rich shales to interpret the tectonic evolution of a depositional basin? *Earth Sci. Rev*., 2008, **86**(1–4), 1–14.
59. Somelar, P., Kirsimäe, K., Hints, R., Kirs, J. Illitization of Early Paleozoic K-Bentonites in the Baltic Basin: decoupling of burial- and fluid-driven processes. *Clay. Clay Miner*., 2010, **58**(3), 388–398.

Presented by J. Boak
Received October 30, 2012